PCCP

RSC Publishing

PAPER

View Article Online
View Journal | View Issue

Cite this: *Phys. Chem. Chem. Phys.*, 2013, **15**, 7512

Importance of temperature on the diffusiophoretic behavior of a charge-regulated zwitterionic particle

Shiojenn Tseng,[a] Ting-Wen Lo,[b] Chien Hsu,[b] Yu-Kui Fu[b] and Jyh-Ping Hsu*[b]

Received 21st January 2013,
Accepted 14th March 2013

DOI: 10.1039/c3cp50264c

www.rsc.org/pccp

Previous theoretical diffusiophoresis analyses were usually based on a fixed temperature, and its influence on the diffusiophoresis behavior of a particle was seldom discussed. Because both the physicochemical properties of the liquid phase and the charged conditions of a particle can be influenced appreciably by the temperature, so is diffusiophoresis behavior. This effect is taken into account in the present study for the first time, along with the possible presence of multiple ionic species in the liquid phase, a factor of practical significance if reactions occur on the particle surface and/or the solution pH is adjusted. Taking an aqueous dispersion of SiO_2 particles as an example, a thorough numerical simulation is conducted to examine the behavior of a charge-regulated, zwitterionic particle subject to an applied salt concentration gradient under various conditions. Considering the potential applications of diffusiophoresis, the results gathered provide necessary information for the design of diffusiophoresis devices, and empirical relationships that correlate the scaled particle mobility with key parameters are developed for that purpose.

1 Introduction

Diffusiophoresis has been applied to both laboratory scaled devices and real scaled operations.[1–8] Abécassis *et al.*, for example, showed experimentally that the rate of diffusion-based migration of 200 nm silica particles can be raised by two orders of magnitude by applying a salt concentration gradient.[9] Diffusiophoresis also has the potential to enhance the particle migration rate driven by other applied fields when they are not sufficiently efficient. For instance, in nanopore-based DNA sequencing, where DNA molecules are driven by an applied electric field, the capture rate of DNA towards the entrance of a nanopore is usually very slow.[10] In this case, it is possible to raise that rate by applying an extra salt concentration gradient.

For a charged particle in an electrolyte (salt) solution, the mechanisms involved in diffusiophoresis include mainly chemiphoresis and electrophoresis.[11–13] The former result from the unbalanced ionic distribution surrounding a particle, or double-layer polarization (DLP). Two types of DLP are present;[14,15] type I DLP, which occurs inside the double layer, drives a particle towards the direction of the applied salt concentration gradient (high-concentration side); type II DLP, which occurs immediately outside the double layer, drives it towards the opposite direction (low-concentration side). The electrophoresis effect needs be considered when the diffusivity of cations differs appreciably from that of anions,[16] such as in the case of an aqueous NaCl solution. Depending upon the sign of the surface charge of a particle, this effect is capable of driving it towards either the high- or low-concentration side.

Many theoretical attempts have been made on modeling the diffusiophoresis of particles under various conditions. Prieve *et al.*,[17] for example, considered the diffusiophoresis of an isolated rigid sphere in an infinite electrolyte solution. Taking account of the particle concentration, Hsu *et al.*[18] studied the diffusiophoresis of spherical particles. Several studies focused on the boundary effect on diffusiophoresis, such as for a sphere in a spherical cavity,[16] a sphere along the axis of a cylindrical pore,[19] and a finite cylinder in a cylindrical pore.[20] The diffusiophoresis of a charged-regulated sphere normal to two parallel disks was investigated by Hsu *et al.*,[21] and that along the axis of a cylindrical pore by Hsu *et al.*[22] Attempts were also made on simulating the diffusiophoresis of non-spherical particles,[23] non-uniformly charged particles,[24,25] and non-rigid particles.[26–28]

Because diffusiophoresis is associated with a salt concentration gradient, the concentrations of all the ionic species in the liquid phase play the key role. Previous analyses almost always assumed that the liquid phase has binary electrolytes only (*i.e.*, one kind of cation and one kind of anion). This can be unrealistic in practice, for example, where a particle is zwitterionic (and therefore, charge-regulated) and the solution pH needs be adjusted. For example, for an aqueous KCl solution with its pH adjusted by KOH and HCl, the presence of at least four kinds of ionic species needs

[a] *Department of Mathematics, Tamkang University, Tamsui, Taipei, 25137, Taiwan*
[b] *Department of Chemical Engineering, National Taiwan University, Taipei, 10617, Taiwan. E-mail: jphsu@ntu.edu.tw; Fax: +886-2-23623040; Tel: +886-2-23637448*

be considered: K^+, Cl^-, H^+, and OH^-, especially when pH deviates appreciably from 7. The temperature is another potentially important factor in diffusiophoresis because both the physical properties of the liquid phase and the charged conditions of the particle surface depend upon this factor. The temperature dependence of the diffusiophoretic behavior of a particle, however, can be profound since the variations in the aforementioned properties with temperature are non-linear, in general.

The diffusiophoresis of a rigid, charge-regulated, zwitterionic sphere in an aqueous solution containing multiple ionic species is analyzed theoretically in this study, taking account of the temperature factor. In particular, the potential advantages of adjusting the temperature for raising the particle mobility are discussed. Taking an SiO_2 particle in an aqueous KCl solution with the pH adjusted by KOH and HCl as an example, the influences of the ionic concentration, the temperature, and the solution pH on the particle mobility are discussed.

2 Theory

Fig. 1 shows the problem considered: the diffusiophoresis of a rigid spherical particle of radius a and surface Ω_p subject to an applied salt concentration gradient ∇n_0. The liquid phase is an aqueous, incompressible Newtonian fluid containing N kinds of ionic species. r, φ, θ are the spherical coordinates adopted with the origin at the particle center. For convenience, a z axis is also defined, and ∇n_0 is in the z direction.

Suppose that the particle has a charged-regulated, zwitterionic surface carrying functional groups AH undergoing the dissociation–association reactions $AOH \Leftrightarrow AO^- + H^+$ and $AOH + H^+ \Leftrightarrow AOH_2^+$ with $K_a = N_{AO^-}[H^+]/N_{AOH}$ and $K_b = N_{AOH_2^+}/N_{AOH}[H^+]$ being respectively the corresponding equilibrium constants. N_{AO^-}, N_{AOH}, and $N_{AOH_2^+}$ are the surface number densities of AO^-, AOH, and AOH_2^+, respectively, and $[H^+]$ is the molar concentration of H^+. Let $N_{total} = N_{AO^-} + N_{AOH} + N_{AOH_2^+}$ be the total surface density of AOH. Suppose that the equilibrium $[H^+]$ follows Boltzmann distribution. Then it can be shown that the particle surface charge density, σ_p, can be expressed as

$$\sigma_P = -FN_{total}\left(\frac{K_a - K_b\left([H^+]_0\exp(-\phi_e)\right)^2}{K_a + [H^+]_0\exp(-\phi_e) + K_b\left([H^+]_0\exp(-\phi_e)\right)^2}\right) \quad (1)$$

Here, ϕ_e, F, and $[H^+]_0$ are the equilibrium electrical potential, Faraday constant, and the bulk H^+ concentration.[29]

Let ϕ, ρ, p, e, k_B, and T be the electrical potential, the space charged density, the pressure, the elementary charge, Boltzmann constant, and the absolute temperature, respectively. $\boldsymbol{v}$, ε, and η are the velocity of fluid, and its permittivity and viscosity, respectively; z_j, n_j, and D_j are the valence, the number concentration, and the diffusivity of ionic species j, respectively, $j = 1,2,\ldots,N$. Then the equations below apply:[18,30]

$$\nabla^2\phi = -\frac{\rho}{\varepsilon} = -\sum_{j=1}^{N} z_j e n_j \quad (2)$$

$$\boldsymbol{J}_j = n_j\boldsymbol{v} - D_j\left(\nabla n_j + \frac{z_j e n_j}{k_B T}\nabla\phi\right) \quad (3)$$

$$\nabla\cdot\boldsymbol{J}_j = 0 \quad (4)$$

$$\nabla\cdot\boldsymbol{v} = 0 \quad (5)$$

$$-\nabla p + \eta\nabla^2\boldsymbol{v} - p\nabla\phi = 0 \quad (6)$$

We assume that the background (equilibrium) concentration field near the particle is influenced only slightly by ∇n_0, that is, $|\nabla n_0| \ll n_{0e}/a$ with n_{0e} being the equilibrium bulk number concentration.[18,30] In this case, each of the dependent variables, ϕ, $\boldsymbol{v}$, p, and n_j can be partitioned into an equilibrium component and a perturbed component as $\phi = \phi_e + \delta\phi$, $\boldsymbol{v} = \boldsymbol{v}_e + \delta\boldsymbol{v}$, $p = p_e + \delta p$, and $n_j = n_{je} + \delta n_j$. The subscript e and the prefix δ denote the equilibrium component and the perturbed component of a variable, respectively, the latter comes from ∇n_0. Because the double layer surrounding the particle might no longer remain symmetric, n_j is expressed as[31]

$$n_j = n_{j0e}\exp\left[-\frac{z_j e\left(\phi_e + \delta\phi + g_j\right)}{k_B T}\right], \quad (7)$$

where g_j and n_{j0e} are a perturbed term taking account of the deformation of double layer and the equilibrium bulk number concentration of ionic species j, respectively. Substituting the partitioned expression for each dependent variable into eqn (2)–(6), we obtain,[16,26] after simplification,

$$\nabla^{*2}\phi_e^* = -\frac{(\kappa a)^2}{\sum_{j=1}^{N}\alpha_{210}}\sum_{j=1}^{N}\alpha_{110}\exp\left(-\alpha_{100}\phi_e^*\right) \quad (8)$$

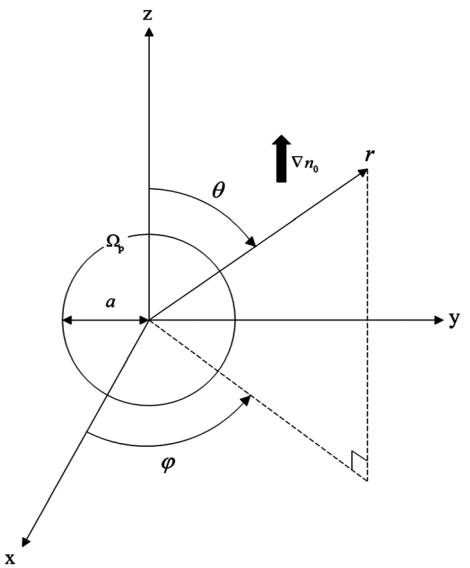

Fig. 1 Diffusiophoresis of a rigid spherical particle of radius a and surface Ω_p subject to an applied salt concentration gradient ∇n_0; r, φ, θ are the spherical coordinates adopted with the origin at the particle center; ∇n_0 is in the z direction.

$$\nabla^{*2}\delta\phi^* = \frac{(\kappa a)^2}{\sum_{j=1}^{N}\alpha_{210}}\sum_{j=1}^{N}\alpha_{210}\left(\delta\phi^* + g_j^*\right)\exp\left[-\alpha_{100}\phi_e^*\right] \quad (9)$$

$$\nabla^{*2}g_j^* - \alpha_{100}\nabla^*\phi_e^*\cdot\nabla^* g_j^* = \gamma \mathrm{Pe}_j \boldsymbol{v}^*\cdot\nabla\phi_e^* \quad (10)$$

$$-\nabla^*\delta p^* + \gamma\nabla^{*2}\boldsymbol{v}^* + \nabla^{*2}\delta\phi^*\nabla^*\phi_e^* + \nabla^{*2}\phi_e^*\nabla^*\delta\phi = 0 \quad (11)$$

$$\nabla^*\cdot\boldsymbol{v}^* = 0 \quad (12)$$

Here, $\nabla^* = a\nabla$, $\nabla^{*2} = a^2\nabla^2$, $\phi_e^* = \phi_e/(k_\mathrm{B}T/z_1e)$, $\delta\phi^* = \delta\phi/(k_\mathrm{B}T/z_1e)$, $n_j^* = n_j/n_{j0e}$, $g_j^* = n_j/n_{j0e}$, $\mathrm{Pe}_j = \varepsilon(k_\mathrm{B}T/z_1e)^2/\mu D_j$, $\kappa = \left[\sum_{j=1}^{2} n_{j0}(ez_j)^2\Big/\varepsilon k_\mathrm{B}T\right]^{1/2}$, $\gamma = \nabla^* n_0^*$, $\boldsymbol{v}^* = \boldsymbol{v}/U^0$, $U_0 = \varepsilon\gamma(k_\mathrm{B}T/z_1e)^2/a\mu$, $j = 1,2,\ldots,N$, and $\delta p^* = \delta p/(\varepsilon\zeta_a{}^2/a^2)$. κ, Pe_j, and U_0 are the reciprocal Debye length, the electric Peclet number of ionic species j, and a reference velocity, respectively; $\alpha_{lmn} = z_j^l n_{j0}^m D_j^n/z_1^l n_{10}^m D_1^n$, where subscript 1 denotes a reference ionic species.

To specify the boundary conditions associated with eqn (8)–(12), we assume the following. (a) The particle surface is non-slip, non-conductive, and impermeable to ionic species. (b) The net ionic flux $\sum_j z_j\boldsymbol{J}_j$ vanishes at a point far away from the particle, with z_j and $\boldsymbol{J}_j$ being the valence and the flux of ionic species j, respectively.[11,16,18] (c) The bulk ionic concentration is $n_{j0e} + z|\nabla n_{j0}|$.[16,18] (d) The liquid phase is stagnant at a point far away from the particle. Therefore, the following boundary conditions apply:

$$\boldsymbol{n}\cdot\nabla^*\phi_e^* = \frac{ae\mathrm{FN}_\mathrm{total}}{\varepsilon k_\mathrm{B}T}\left(\frac{K_\mathrm{a} - K_\mathrm{b}\left([\mathrm{H}^+]_0\exp\left(-\phi_e^*\right)\right)^2}{K_\mathrm{a} + [\mathrm{H}^+]_0\exp\left(-\phi_e^*\right) + K_\mathrm{b}\left([\mathrm{H}^+]_0\exp\left(-\phi_e^*\right)\right)^2}\right) \quad \text{on} \quad \Omega_\mathrm{p} \quad (13)$$

$$\boldsymbol{n}\cdot\nabla^*\delta\phi^* = 0 \quad \text{on} \quad \Omega_\mathrm{p} \quad (14)$$

$$\boldsymbol{n}\cdot\nabla^* g_j^* = 0 \quad \text{on} \quad \Omega_\mathrm{p} \quad (15)$$

$$\boldsymbol{v}^* = 0 \quad \text{on} \quad \Omega_\mathrm{p} \quad (16)$$

$$\boldsymbol{n}\cdot\nabla^*\phi_e^* = 0 \quad \text{as} \quad r^* \to \infty \quad (17)$$

$$\boldsymbol{n}\cdot\nabla^*\delta\phi^* = -\gamma\frac{(D_1 - D_2)}{D_1\sum_{j=1}^{4}\alpha_{211}}\cos\theta \quad \text{as} \quad r^* \to \infty \quad (18)$$

$$g_1^* = -r^*\cos\theta\gamma - \delta\phi^* \quad \text{as} \quad r^* \to \infty \quad (19)$$

$$g_2^* = \frac{1}{\alpha_{100}}r^*\cos\theta\gamma - \delta\phi^* \quad \text{as} \quad r^* \to \infty \quad (20)$$

$$g_3^* = -\delta\phi^* \quad \text{as} \quad r^* \to \infty \quad (21)$$

$$g_4^* = -\delta\phi^* \quad \text{as} \quad r^* \to \infty \quad (22)$$

$$\boldsymbol{v}^* = -U\cos\theta\boldsymbol{e}_\mathrm{r} \quad \text{as} \quad r^* \to \infty \quad (23)$$

In these expressions, $r^* = r/a$; $\boldsymbol{n}$ and $\boldsymbol{e}_r$ are the unit outer normal vector and the unit vector in the r direction, respectively.

Instead of solving the present problem directly, an approach similar to that of O'Brien and White[31] in electrophoresis analysis is adopted. We partition the original problem into two sub-problems.[18,30] In the first sub-problem, ∇n_0 is not applied but the particle moves with a constant velocity U, and ∇n_0 is applied but the particle is held fixed in the second sub-problem. Let $\boldsymbol{F}_i$ be the total force acting on the particle in the z direction in sub-problem i and F_i be its magnitude. Then $F_1 = \chi_1 U$ and $F_2 = \chi_2\,\nabla n_0$, where χ_1 and χ_2 are constant. Because we assume that the system is in a pseudo steady state, $F_1 + F_2 = 0$, yielding

$$U = \frac{-\chi_2\nabla n_0}{\chi_1} \quad (24)$$

In our case the forces acting on the particle include the electric force $\boldsymbol{F_e}$ and the hydrodynamic force $\boldsymbol{F_d}$. Let F_{ei} and F_{di} be the z components of $\boldsymbol{F_e}$ and $\boldsymbol{F_d}$ in sub-problem i, respectively, with $F_{di}^* = F_{di}/\varepsilon(k_\mathrm{B}T/z_1e)^2$ and $F_{ei}^* = F_{ei}/\varepsilon(k_\mathrm{B}T/z_1e)^2$ being the corresponding scaled forces. Then F_{ei} and F_{di} can be evaluated by[32]

$$F_{ei}^* = \int_{S^*}\left(\frac{\partial\phi_e^*}{\partial n}\frac{\partial\delta\phi^*}{\partial z} - \frac{\partial\phi_e^*}{\partial t}\frac{\partial\delta\phi^*}{\partial t}\right)\mathrm{d}\Omega_\mathrm{p}^* \quad (25)$$

$$F_{di}^* = \int_{S^*}\left(\boldsymbol{\sigma}^{\boldsymbol{H}*}\cdot\boldsymbol{n}\right)\cdot\boldsymbol{e}_z\mathrm{d}\Omega_\mathrm{p}^* \quad (26)$$

Here, $\Omega_\mathrm{p}^* = \Omega_\mathrm{p}/a^2$ is the scaled particle surface area; $\partial/\partial n$ and $\partial/\partial t$ are the rate of change with distance along $\boldsymbol{n}$ and the unit tangential vector $\boldsymbol{t}$, respectively; $\boldsymbol{\sigma}^{\boldsymbol{H}^*} = \boldsymbol{\sigma}^{\boldsymbol{H}}/\varepsilon(k_\mathrm{B}T/z_1e)^2$ is the scaled shear stress tensor with $\boldsymbol{\sigma}^{\boldsymbol{H}}$ being the corresponding shear stress tensor.

3 Results and discussion

3.1 Code verification

The present problem is solved numerically by FlexPDE,[33] a finite element method based commercial software. Its applicability is first verified by applying it to solving the diffusiophoresis of an isolated rigid sphere of constant surface potential at a fixed temperature. This problem was solved numerically for an arbitrary level of particle surface potential,[15] and analytically at a low surface potential.[34] Fig. 2 summarizes the variation of the scaled diffusiophoretic mobility U^* with the absolute value of the scaled particle surface potential $|\phi_\mathrm{s}^*|$. This figure shows that our results are close to those of Prieve *et al.*[15] for the range of $|\phi_\mathrm{s}^*|$ examined. The deviation of the results of Keh and Wei[34] from ours at high levels of $|\phi_\mathrm{s}^*|$ is expected because their analysis is valid only at a low $|\phi_\mathrm{s}^*|$.

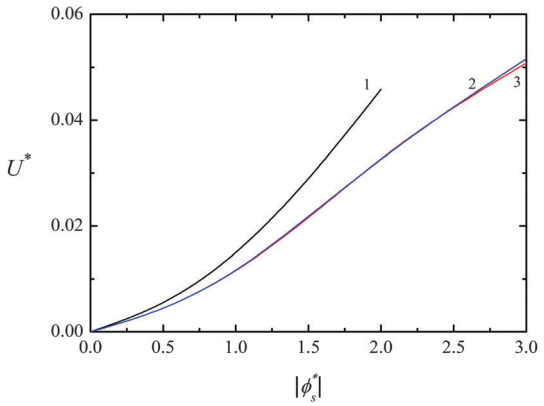

Fig. 2 Variation of the scaled mobility U^* with the absolute value of the scaled particle surface potential $|\phi_s^*|$ at κa= 1; curve 1, analytical result of Keh and Wei;[34] 2, numerical result of Prieve and Roman;[17] 3, present result.

3.2 Numerical simulation

To examine the diffusiophoretic behavior of a particle under various conditions, we conduct a series of numerical simulations by varying the solution pH, the background salt concentration, and the temperature. In our case, ε, η, D_j, K_a, and K_b are all temperature dependent, as is the equilibrium dissociation constant of water, K_w. For illustration, we consider the case where an SiO_2 particle with $N_{total} = 5 \times 10^{-6}$ mol m^{-2}, pK_a = 7 and pK_b = 2 (ref. 35 and 36) is immersed in an aqueous KCl solution,[35,36] the solution pH is adjusted by HCl and KOH, and a KCl concentration gradient is applied. In this case, the presence of K^+, Cl^-, H^+, and OH^- might all be significant. For simplicity, we assume that the liquid phase is a relatively dilute solution with its physical properties essentially the same as those of pure water. Therefore, the following expressions are adopted:[37–41]

$$D_j = \frac{RT}{F^2}\left[\frac{1/|z_j|}{1/\lambda_j^0}\right] \quad (27)$$

$$\ln K_a = -\frac{\Delta_r G^0}{k_B T} \quad (28)$$

$$\log(\eta/T^{1.5}) = a_1 + a_2 x + a_3 x^2 + a_4 x^3 \quad (29)$$

$$\ln \varepsilon = -\ln \varepsilon(0,0) + 2[b_1\tau + b_2\tau\omega + b_3\tau\omega^2 + b_4\tau^2 + b_5\tau^2\omega + b_6\tau^2\omega^2 + b_7\omega + b_8\omega^2] \times 10^{-6} \quad (30)$$

$$K_w = 8.754 \times 10^{-10} \exp(-1.01 \times 10^6/T^2) \quad (31)$$

Here, R and λ_j^0 are gas constant and the limiting conductance of ionic species j, respectively. The limiting conductance of H^+, K^+, Cl^-, and OH^- is 349.6, 76.31, 76.31, and 198.0 S cm^2 mol^{-1}, respectively. For simplicity, the temperature dependence of λ_j^0 is neglected. $\Delta_r G^0$ ($\cong$13.4 kcal mol^{-1}) is the standard Gibbs free energy for the reaction AOH $\Leftrightarrow$ AO^- + H^+.[37] The units of η in eqn (29) are kg m^{-1} s^{-1}; $a_1 = -5.26$, $a_2 = 4.59$, $a_3 = 1.32$, $a_4 = 0.15$;[38] $x = 10^3/T$(K); $b_1 = -22.57$, $b_2 = -3.21 \times 10^{-2}$, $b_3 = -2.85 \times 10^{-4}$, $b_4 = -1.18 \times 10^{-3}$, $b_5 = 2.79 \times 10^{-5}$, $b_6 = -1.48 \times 10^{-7}$, $b_7 = 2.30 \times 10^3$, $b_8 = -0.13$.[39] τ is the gage pressure (Pa), which is zero in our case; $\omega = T - 273$ is in °C. $\varepsilon = \varepsilon_r\varepsilon_0$ with ε_0 (Coul^2 N^{-1} m^{-2}) being the dielectric constant of a vacuum. $\varepsilon_r(0,0)$ ($\cong$87.88) is the relative permittivity of water at $\omega = 0$ and $\tau = 0$. The ranges of T in eqn (29)–(31) are $273 < T(K) < 373$, $273 < T(K) < 343$, and $273 < T(K) < 333$, respectively. For the range of pH considered, 4 to 8, because the association reaction $AOH_2^+ \Leftrightarrow AOH + H^+$ is essentially complete, the temperature dependence of K_b can be neglected.

3.3 Influence of pH and T on ϕ_s

Fig. 3 shows the dependence of the particle surface potential ϕ_s on the solution pH at various levels of the temperature T. For the range of pH considered, 4 to 8, the double layer thickness is roughly constant at $\kappa a \cong 2$. In addition, the particle surface is negatively charged with its charge density depending upon the degree of dissociation of AH, which is closely related to both pH and T. As can be seen in Fig. 3, $|\phi_s|$ increases with increasing pH and T. The former is because a higher pH is advantageous to the dissociation of AH, yielding a higher surface charge density. The latter is expected because a higher T yields a larger K_a and, therefore a higher degree of dissociation of AH.

3.4 Influence of pH and T on U^*

Fig. 4 illustrates the variation in the scaled particle mobility U^* with the solution pH and the temperature T. Fig. 4a suggests that U^* is positive, except at a high pH. As shown in Fig. 4b, for a fixed T, U^* has a local maximum occurring at $6 < pH < 7$, and as T increases, the pH at which the local maximum of U^* occurs shifts to a lower value. The presence of that local maximum arises from the competition between the effect of DLP[16] and that of the hydrodynamic retardation flow resulting from the osmotic flow due to the unbalanced ionic distribution. As mentioned previously, $|\phi_s|$ increases with increasing pH, implying that both the significance of osmotic flow and that of type II DLP increase accordingly. If pH is lower than *ca.* 6, U^* is dominated by type I DLP, and therefore, it increases with increasing pH. Note that the curves corresponding to various values of T do not cross at the same point, as illustrated by the

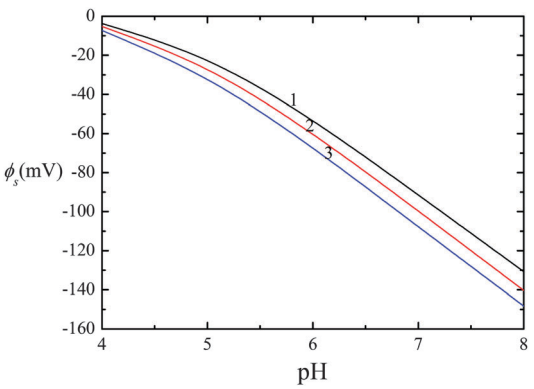

Fig. 3 Variations of the particle surface potential ϕ_s with pH and three levels of T at a = 20 nm, pK_a = 7, pK_b = 2, $N_{total} = 5 \times 10^{-6}$ mol m^{-2}, and $C_{KCl} = 10^{-3}$ M; curve 1, T = 298 K; 2, T = 303 K; 3, T = 308 K.

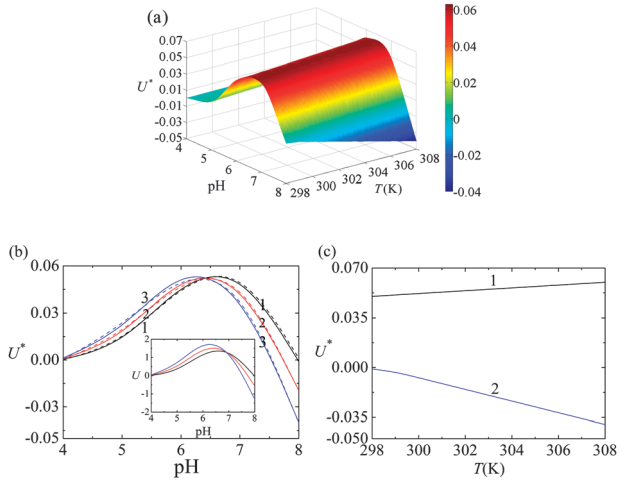

Fig. 4 (a) Variation of the scaled mobility U^* with pH and T at a = 20 nm, pK_a = 7, pK_b = 2, $N_{total} = 5 \times 10^{-6}$ mol m^{-2}, and $C_{KCl} = 10^{-3}$ M; (b) variation of U^* with pH and three levels of T; curve 1, T = 298 K; 2, T = 303 K; 3, T = 308 K; insert: corresponding variation in U (10^{-12} m^2 s^{-1} M^{-1}); (c) variation of U^* with T and two levels of pH; curve 1, pH 6; 2, pH 8.

insert in Fig. 4b, where U is plotted. As exemplified in Fig. 4c, $U^* > 0$ for the case considered, and it increases with increasing T, which can be attributed to the increase in the equilibrium constants and, therefore, the surface potential. However, if pH exceeds *ca.* 7, because the effect of type I DLP is offset by that of type II DLP, the effect of osmotic flow dominates, and U^* decreases with increasing pH so that U^* shows a local maximum. As seen in Fig. 4c, $U^* < 0$, and $|U^*|$ increases with increasing T. Again, this can be attributed to the increase in the equilibrium constant and, therefore, the surface potential.

Fig. 5 shows the variations in the scaled perturbed ionic concentrations, $\delta n_1 = n_{cation} - n_{cation,e}$ and $\delta n_2 = n_{anion} - n_{anion,e}$, as a function of the scaled distance along the z axis, $Z = z/a$, on the plane $\varphi = \pi/2$ for the case of Fig. 4. Here, n_{cation} and n_{anion} are the number concentrations of cations (K^+, H^+) and anions (Cl^-, OH^-), respectively, and $n_{cation,e}$ and $n_{anion,e}$ are the corresponding equilibrium concentrations, respectively. The particle in Fig. 5a is negatively charged. In this case, δn_1 is seen to be positive (negative) on the high- (low-) concentration side, exemplifying the presence of type I DLP.[18] This generates a local electric field driving the particle towards the high-concentration side. Fig. 5b indicates that immediately outside the double layer, $\delta n_1 < \delta n_2$ ($\delta n_1 > \delta n_2$) on the high- (low-) concentration side, known as type II DLP,[16] which drives the particle towards the opposite direction to that of the applied concentration gradient. If pH is low, U^* increases with increasing pH, which is expected because the higher the pH the higher the particle surface potential, as seen in Fig. 3. This also implies that the higher the pH the more significant the type I DLP is. Note that for pH < 6, the effect of type I DLP is more important than that of hydrodynamic retardation flow, which drives the particle towards the low-concentration side. However, if pH is sufficiently high, because type II DLP becomes significant, the driving force coming from type I DLP is offset appreciably so that hydrodynamic retardation flow dominates. In this case, the particle mobility becomes negative (*i.e.*, it is driven to the low-concentration side).

The contours of the scaled velocity on the plane $\varphi = \pi/2$ for the case of Fig. 4 are presented in Fig. 6, where $R = r/a$. The fluid inside the double layer is driven by the electric field associated with type I DLP. The fluid flow at pH 8 is more appreciable than that at pH 5 due to a more unbalanced ionic distribution, as shown in Fig. 5.

A regression analysis on the results shown in Fig. 4a yields

$$\begin{aligned} U^* = {} & (1.67000 \times 10^{-6}\, T - 8.86677 \times 10^{-3})\mathrm{pH}^3 \\ & + (-7.25720 \times 10^{-4}\, T + 0.35503)\mathrm{pH}^2 \\ & + (7.47691 \times 10^{-3}\, T - 2.95581)\mathrm{pH} \\ & + (-1.83683 \times 10^{-2}\, T + 6.69993), \end{aligned} \quad (32)$$

where T is in K, with a correlation coefficient of 0.9944. The dashed curves in Fig. 4b denote the results based on this expression.

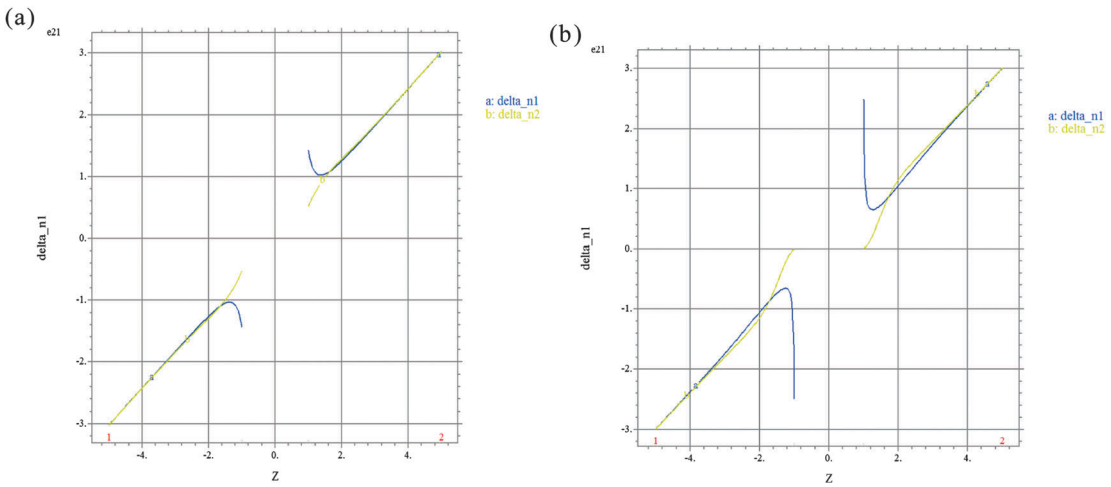

Fig. 5 Variations in the scaled perturbed ionic concentrations $\delta n_1 = n_{cation} - n_{cation,e}$ and $\delta n_2 = n_{anion} - n_{anion,e}$ with the scaled distance along the z axis, $Z = z/a$, on the plane $\varphi = \pi/2$ at a = 20 nm, pK_a = 7, pK_b = 2, $N_{total} = 5 \times 10^{-6}$ mol m^{-2}, and $C_{KCl} = 10^{-3}$ M; (a) pH 5, (b), pH 8.

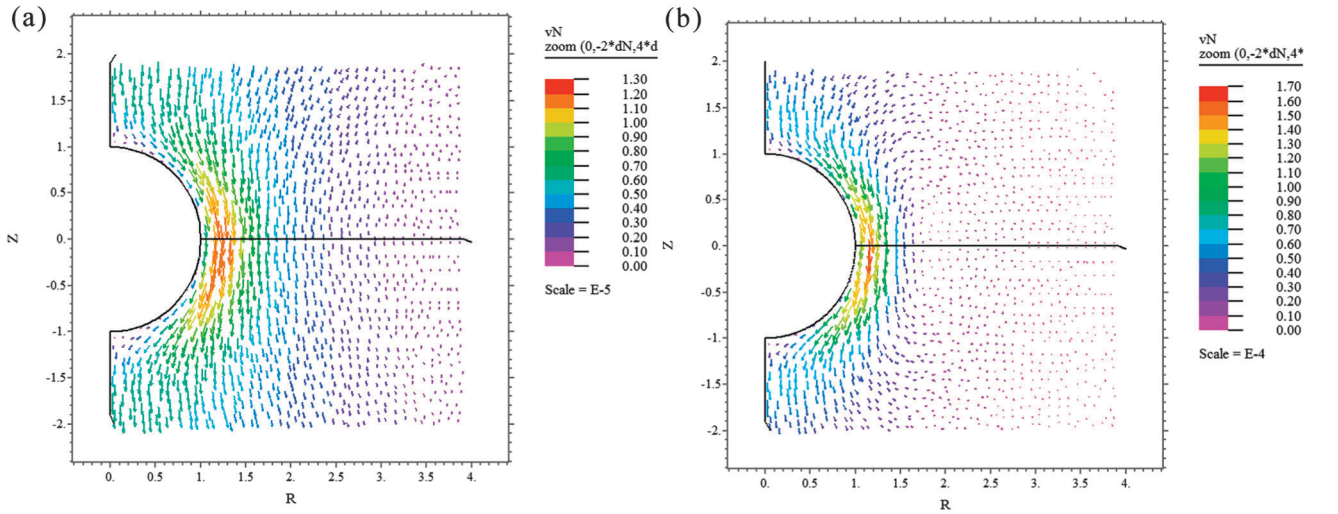

Fig. 6 Contours of the scaled velocity on the plane $\varphi = \pi/2$ for the case in Fig. 5.

3.5 Influence of C_{KCl} and T on U^*

Fig. 7 and 8 summarize the influences of the background concentration C_{KCl} and the temperature T on the scaled diffusiophoretic velocity U^* at two representative levels of pH. Fig. 7a reveals that at pH 6, U^* has a local maximum as C_{KCl} varies, which results from the competition between type I and type II DLP.[16] For a fixed value of T, if C_{KCl} is low, U^* increases with increasing C_{KCl}, as illustrated by Fig. 7b. This is because a higher C_{KCl} implies a larger κa, a higher concentration of counterions inside the double layer and, therefore, a more significant type I DLP. However, an increase in κa also implies a stronger type II DLP electric field, especially when κa is large and the surface potential is high. Therefore, if κa is sufficiently large, the effect of type I DLP is offset by that of type II DLP. In this case, U^* might decrease with increasing C_{KCl}. As seen in Fig. 7c, for a fixed level of C_{KCl}, the higher the T the larger the

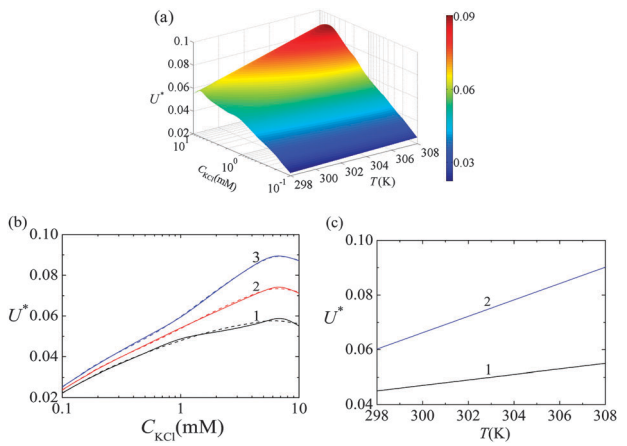

Fig. 7 (a) Variation of the scaled mobility U^* with C_{KCl} and T at a = 20 nm, $pK_a = 7$, $pK_b = 2$, $N_{total} = 5 \times 10^{-6}$ mol m^{-2}, and pH 6; (b) variation of U^* with C_{KCl} at three levels of T; curve 1, T = 298 K; 2, T = 303 K; 3, T = 308 K; dashed curves: results based on eqn (33); (c) variation of U^* with T at two levels of C_{KCl}; curve 1, $C_{KCl} = 0.7 \times 10^{-3}$ M; 2, $C_{KCl} = 7 \times 10^{-3}$ M.

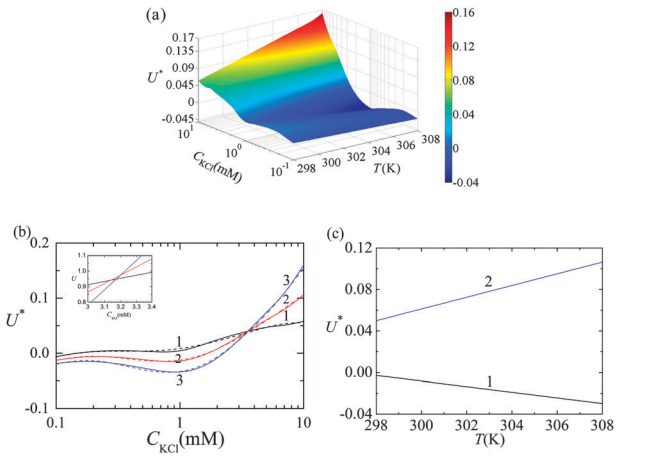

Fig. 8 (a) Variation of the scaled mobility U^* with C_{KCl} and T at a = 20 nm, $pK_a = 7$, $pK_b = 2$, $N_{total} = 5 \times 10^{-6}$ mol m^{-2}, and pH 8; (b) variation of U^* with C_{KCl} at three levels of T; curve 1, T = 298 K; 2, T = 303 K; 3, T = 308 K; insert: corresponding variation in U (10^{-12} m^2 s^{-1} M^{-1}); dashed curves: results based on eqn (34); (c) variation of U^* with T at two values of C_{KCl}; curve 1, $C_{KCl} = 0.7 \times 10^{-3}$ M; 2, $C_{KCl} = 7 \times 10^{-3}$ M.

U^*. Similar to the case of Fig. 4c, this is because the higher the temperature the larger the equilibrium constant, and therefore, the higher the particle surface potential.

Fig. 8 indicates that the behavior of U^* at pH 8 is more complicated than at pH 6. This is because the surface potential is much higher in the former, as mentioned in the discussion of Fig. 2. Fig. 8b shows that, unless C_{KCl} is sufficiently high, U^* is negative. This is because as C_{KCl} increases from a low value, type II DLP dominates, and the particle tends to move towards the low-concentration side. However, for a fixed pH, if C_{KCl} is sufficiently high, the larger the κa the lower the surface potential, and therefore, the weaker the electric field associated with type II DLP. In this case, the particle movement is dominated by type I DLP, which drives it towards the high-concentration side. Similar to the case of Fig. 4b, the curves do

not cross at the same point. Fig. 8c shows that if C_{KCl} is low, $|U^*|$ increases with increasing T. This is because the higher the T the stronger the electric field associated with type II DLP, as mentioned in the discussion of Fig. 4c. However, if C_{KCl} exceeds a certain level, because the degree of type II DLP decreases due to the decay in the particle surface potential, type I DLP dominates, and U^* increases with the increase in T.

The results shown in Fig. 7a and 8a can be expressed respectively by

$$\begin{aligned} U^* = {} & (-1.46879 \times 10^{-3}\, T + 0.43224)\beta^4 \\ & + (-8.22530 \times 10^{-4}\, T + 0.24287)\beta^3 \\ & + (2.04816 \times 10^{-3}\, T - 0.61369)\beta^2 \\ & + (2.23430 \times 10^{-3}\, T - 0.64663)\beta \\ & + 1.12506 \times 10^{-3}\, T - 0.28726, \end{aligned} \tag{33}$$

and

$$\begin{aligned} U^* = {} & (-2.53723 \times 10^{-3}\, T + 0.71251)\beta^4 \\ & + (6.18957 \times 10^{-3}\, T - 1.84362)\beta^3 \\ & + (1.1280 \times 10^{-2}\, T - 3.29972)\beta^2 \\ & + (-6.04060 \times 10^{-4}\, T + 0.21020)\beta \\ & - 4.49422 \times 10^{-3}\, T + 1.34593, \end{aligned} \tag{34}$$

where $\beta = \log(C_{KCl} \times 10^3)$. The correlation coefficients based on eqn (33) and (34) are 0.9980 and 0.9958, respectively.

It should be emphasized that considering multiple ionic species might yield diffusiophoretic behaviors that are different both quantitatively and qualitatively from those when two kinds of ionic species are considered only. This is because all the ionic species in the liquid phase contribute to the double layer thickness, which is one of the key factors in diffusiophoresis, and neglecting the presence of several ionic species will overestimate that thickness. In addition, if the background concentration is low, both type I and type II DLP can be influenced significantly by the polarization of H^+ and OH^- induced by the local electric fields established by those DLPs, as are the diffusiophoretic behaviors of a particle.

In general, as the temperature increases, both the viscosity and the permittivity of the liquid phase decrease, but the ionic diffusivity increases. A decrease in the viscosity yields a decrease in hydrodynamic drag acting on the particle which, therefore, raises its mobility. The mobility increases with increasing ionic diffusivity. This is because a higher diffusivity yields a smaller Peclet number so that the convective term on the right-hand side of eqn (10) is smaller, implying that the relaxation effect is less significant. However, it is difficult to predict the influence of the permittivity on the mobility because the double layer thickness is influenced by the former. As illustrated in the results of numerical simulation, the mobility depends complicatedly on that thickness.

4 Conclusions

We investigated theoretically the influence of the solution pH, the temperature T, and the background salt concentration on the diffusiophoresis of a rigid, charge-regulated zwitterionic spherical particle. This extends the conventional diffsiophoresis analyses to a more general and realistic case, where the particle surface is not necessarily maintained either at a constant potential or at a constant charge density, the liquid phase might contain multiple ionic species, and T might vary. Adopting an SiO_2 particle in an dilute aqueous KCl solution, the pH of which is adjustable by HCl and KOH, as an example, we show that the competition of two types of double-layer polarization (DLP) and osmotic flow, all due to the unbalanced ionic distribution, yields the following interesting and important results. (i) For the ranges of pH and T considered, 4 to 8 and 298 to 308 K, respectively, the absolute value of the particle surface potential increases with increasing pH and T due to a higher degree of dissociation of the acidic functional groups. This implies that as pH and T increase, both the significance of DLP and that of osmotic flow are enhanced. (ii) The particle mobility increases monotonically with T, in general. (iii) Depending upon the level of pH, the mobility is dominated by DLP or osmotic flow: at low (high) pH, DLP (osmotic flow) dominates, and the mobility increases (decreases) with increasing pH. (iv) The previous conclusion implies that the mobility has a local maximum as pH varies, and the higher the T the lower the pH at which the local maximum occurs. This is because the higher the T the more significant type II DLP is, which offsets the influence of type I DLP. (v) As the background concentration C_{KCl} varies, the mobility is dominated either by type I or type II DLP. If pH is low, type I DLP becomes more significant as C_{KCl} increases from a low value and, therefore, the mobility increases with increasing C_{KCl}. If C_{KCl} reaches a certain level, the effect of type I DLP is offset by that of type II DLP, yielding a local maximum in the mobility. (vi) If pH is high, due to the enhancement in type II DLP, the absolute value of the mobility increases with increasing C_{KCl}. However, if C_{KCl} is sufficiently high, due to the decay in the particle surface potential, type I DLP dominates and, therefore, the mobility increases with increasing C_{KCl}.

Acknowledgements

This work is supported by the National Science Council of the Republic of China.

References

1 A. Meisen, A. J. Bobkowicz, N. E. Cooke and E. J. Farkas, *Can. J. Chem. Eng.*, 1971, **49**, 449.
2 D. C. Prieve, *Nat. Mater.*, 2008, **7**, 769.
3 Z. R. Ul'berg, N. N. Ivzhenko, G. L. Dvornichenko, R. O. Buadze and S. A. Koniashvili, *Ukr. Khim. Zh.*, 1992, **58**, 390.
4 A. A. Korotkova and B. V. Deryagin, *Colloid J. USSR*, 1991, **53**, 719.
5 A. B. Yamenko and D. V. Sednev, *Colloid J.*, 1995, **57**, 396.
6 G. M. Hidy and J. R. Brock, *Environ. Sci. Technol.*, 1969, **3**, 563.

7 Y. Kousaka and Y. J. Endo, *J. Aerosol Sci.*, 1993, **24**, 611.
8 M. Ibele, T. E. Malouk and A. Sen, *Angew. Chem., Int. Ed.*, 2009, **48**, 3308.
9 B. Abécassis and C. Cottin-Bizonne, *Nat. Mater.*, 2008, **7**, 785.
10 M. Zhang, L. H. Yeh, S. Qian, J. P. Hsu and S. W. Joo, *J. Phys. Chem. C*, 2012, **116**, 4793.
11 J. P. Ebel, J. L. Anderson and D. C. Prieve, *Langmuir*, 1988, **4**, 396.
12 S. S. Dukhin, E. S. Malkin and A. S. Dukhin, *Colloid J. USSR*, 1978, **40**, 536.
13 S. S. Dukhin, E. S. Malkin and A. S. Dukhin, *Colloid J. USSR*, 1979, **41**, 734.
14 X. G. Zhang, W. L. Hsu, J. P. Hsu and S. J. Tseng, *J. Phys. Chem. B*, 2009, **113**, 8646.
15 D. C. Prieve, J. L. Anderson, J. P. Ebel and M. E. Lowell, *J. Fluid Mech.*, 1984, **148**, 247.
16 J. P. Hsu, W. L. Hsu and Z. S. Chen, *Langmuir*, 2009, **25**, 1772.
17 D. C. Prieve and R. J. Roman, *J. Chem. Soc., Faraday Trans. 2*, 1987, **83**, 1287.
18 J. P. Hsu, Y. Y. Lou and E. J. Lee, *J. Phys. Chem. B*, 2007, **111**, 2533.
19 J. P. Hsu, W. L. Hsu, M. H. Ku, Z. S. Chen and S. Tseng, *J. Colloid Interface Sci.*, 2010, **342**, 598.
20 J. P. Hsu, I. F. Ko and S. Tseng, *J. Phys. Chem. C*, 2012, **116**, 4455.
21 J. P. Hsu, K. L. Liu, W. L. Hsu, L. H. Yeh and S. J. Tseng, *J. Phys. Chem. B*, 2010, **114**, 2766.
22 J. P. Hsu, W. L. Hsu and K. L. Liu, *Langmuir*, 2010, **26**, 8648.
23 J. P. Hsu, X. C. Luu and W. L. Hsu, *J. Phys. Chem. B*, 2010, **114**, 8043.
24 X. C. Luu, J. P. Hsu and S. Tseng, *J. Chem. Phys.*, 2011, **134**, 064708.
25 J. P. Hsu, X. C. Luu and S. Tseng, *J. Phys. Chem. C*, 2011, **115**, 12592.
26 J. P. Hsu, K. L. Liu, W. L. Hsu, L. H. Yeh and S. Tseng, *Langmuir*, 2010, **26**, 16037.
27 W. L. Hsu, J. P. Hsu and S. Tseng, *Chem. Eng. Sci.*, 2011, **66**, 2199.
28 K. L. Liu, J. P. Hsu, W. L. Hsu, L. H. Yeh and S. Tseng, *Electrophoresis*, 2011, **32**, 3053.
29 J. P. Hsu and Y. H. Tai, *Langmuir*, 2010, **26**, 16857.
30 J. Lou and E. Lee, *J. Phys. Chem. C*, 2008, **112**, 2584.
31 R. W. O'Brien and L. R. White, *J. Chem. Soc., Faraday Trans. 2*, 1978, **74**, 1607.
32 J. P. Hsu, L. H. Yeh and M. H. Ku, *J. Colloid Interface Sci.*, 2007, **305**, 324.
33 *FlexPDE Version 2.22*, PDE Solutions Inc., USA, 2000.
34 H. J. Keh and Y. K. Wei, *Langmuir*, 2000, **16**, 5289.
35 J. Sonnefeld, M. Löbbus and W. Vogelsberger, *Colloids Surf., A*, 2001, **195**, 215.
36 J. P. Hsu, Y. H. Tai, L. H. Yeh and S. Tseng, *J. Phys. Chem. B*, 2011, **115**, 3972.
37 J. Sefcik and W. A. Goddard, *Geochim. Cosmochim. Acta*, 2001, **65**, 4435.
38 P. M. Kampmeyer, *J. Appl. Phys.*, 1952, **23**, 99.
39 B. B. Owen, R. C. Miller, C. E. Miller and H. L. Cogan, *J. Phys. Chem.*, 1961, **65**, 2065.
40 B. E. Poling, J. M. Prausnitz and J. P. O'Connell, *The Properties of Gases Liquids*, McGraw-Hill, New York, 2001.
41 P. A. Stewart, *How to Understand Acid-Base*, Elsevier, New York, 1981.